

*This work deals with fluid-structure interaction (FSI), one of the emerging areas of numerical simulation and calculation. This research shows a numerical study investigating heat transfer enhancement and fluid-structure interaction in a circular finned tube by using alumina nanofluid as a working fluid with a typical twisted tape that has a twisting ratio of 1.85. The studied nanofluid volumes of fraction are =0, 3, 5 % under conditions of laminar and turbulent flow. The solution for such problems is based on the relations of continuum mechanics and is mostly done with numerical methods. FSI occurs when the flow of fluid influences the properties of a structure or vice versa. It is a computational challenge to deal with such problems due to complexity in defining the geometries, nature of the interaction between a fluid and solid, intricate physics of fluids and requirements of computational resources. CFD investigations were made based on the numerical finite volume techniques to solve the governing three-dimensional partial differential equations to get the influence of inserted twisted tape and concentration of nanofluid on heat transfer enhancement, friction loss, average Nusselt number, velocity profile, thermal performance factor characteristics, and two-way interaction in a circular tube at laminar and turbulent flow. The governing continuity, momentum and energy transfer equations are solved using Ansys Fluent and Transient Structural. The simulation results show that the deformations of two-way coupling fluctuate from side to side, with 0.004 mm, as maximum amplitude, located at the typical twisted tape center. Heat transfer dissipation improved by adding fins and as Reynolds numbers increase the heat transfer behavior increases*

**Keywords:** *two-way fluid-structure interaction, CFD, nanofluid, typical twisted tape, finned tube*

# TWO-WAY FLUID-STRUCTURE INTERACTION STUDY OF TWISTED TAPE INSERT IN A CIRCULAR TUBE HAVING INTEGRAL FINS WITH NANOFLUID

**Mustafa Abdulsalam Mustafa\***

**Atheer Raheem Abdullah**

Assistant Lecturer\*

**Wajeeh Kamal Hasan**

Assistant Professor\*

**Laith J. Habeeb**

Assistant Professor

Training and Workshop Center

University of Technology

52 str., Baghdad, Iraq, 10001

**Maadh Fawzi Nassar**

Corresponding author

Postgraduate Student

Department of Chemistry

Universiti Putra Malaysia

Serdang, Selangor, Malaysia, 43400

E-mail: nassarmaadh@gmail.com

\*Department of Refrigeration and Air Conditioning Engineering

Al-Rafidain University College

Palestine str., Baghdad, Iraq, 10001

Received date 16.03.2021

Accepted date 04.06.2021

Published date 30.06.2021

**How to Cite:** Mustafa, M. A., Abdullah, A. R., Hasan, W. K., Habeeb, L. J., Nassar, M. F. (2021). Two-way fluid-structure interaction study of twisted tape insert in a circular tube having integral fins with nanofluid. *Eastern-European*

*Journal of Enterprise Technologies*, 3 (8 (111)), 25–34. doi: <https://doi.org/10.15587/1729-4061.2021.234125>

## 1. Introduction

Fluid-structure interaction (FSI) is a multi-physics phenomenon, which occurs in a system where a flow of fluid causes a solid structure to deform, which, in turn, changes the boundary condition of a fluid system. This kind of interaction occurs in many natural phenomena and man-made engineering systems. It becomes a crucial consideration in the design and analysis of various engineering systems. In fact, it has a great role in heat transfer processes. FSI problems play prominent roles in many scientific and engineering fields, yet a comprehensive study of such problems remains a challenge due to their strong nonlinearity and multidisciplinary nature.

The method to augment heat transfer performance is referred to as heat transfer enhancement, intensification or augmentation. Heat transfer by convection increased by augmentation techniques reduces the heat exchanger thermal resistance. Heat transfer enhancement techniques cause an increase in the coefficient of heat transfer and pressure

drop. When using any of these techniques to design a heat exchanger, the pressure drop and heat transfer rate analysis has to be performed [1]. Nowadays, engineering researchers are looking for new enhancement methods for transferring heat between surfaces and ambient fluid. By this fact, the researcher [2–4] classified the mechanisms of improving convective heat transfer for active or passive techniques.

Passive techniques do not need an outside energy input, not include the use of swirl flow devices, displaced promoters, extended surfaces, roughened surfaces, and blower power or pump to move the fluid, amongst some others. Active techniques, on the other hand, need extra power to affect the process to enhance convective heat transfer [5]. The latter is called a hybrid technique and it is a combination of the previous techniques. Hybrid heat transfer techniques are a combined augmentation of two or more techniques applied at the same time to produce an improvement that is larger than when applying techniques separately. This technique has limited applications and includes complex designs [2]. A few examples of compound techniques are a twisted tape

insert in an internally finned tube, acoustic vibrations with a rough cylinder, and twisted tape with a rough tube wall, fins and electric fields.

Twisted tapes are strips made of metal twisted to a desired shape and dimensions using a suitable technique, inserted in the way of the flow. It is a widespread technique used in heat exchangers to improve the heat transfer rate and reduce the friction factor as a second advantage, which reduces the penalty on pumping power [6]. However, if it is inserted with clearance, it neglects the fin job, and the swirling flow will not be achieved. The clearance may also damage tubes because the tape repeatedly hits the wall. On the other hand, if it is too tight, the tapes' insertion will be too hard. Inserted twisted tapes make a swirl flow and disrupt the thermal boundary layer on the tube wall due to continuous change in the surface geometry along with the flow, enhancing the convective heat transfer. The effect of twisted tape is to make superimposed vortex motion (swirl flow) and turbulence in a flow with a thinner boundary layer, due to continuous changes in the tape geometry, leading to an increase in the heat transfer coefficient and Nusselt number [7]. Despite, the pressure drop will be increased inside the tube by the effect of the tape insert. Therefore, several researchers investigated the optimal design experimentally and numerically and got a high thermal performance with low friction losses.

Modern technology to improve the heat transfer process is called nanotechnology. This technology enabled nanoparticles production with a particle size below 100 nm. Nanoparticles have higher thermal properties than those of bulk materials of the same composition [8]. Nanofluid is nanoparticles mixed with a base fluid, which have the ability to transfer more heat than conventional heat fluid such as water, ethylene glycol and oil [9] with their superior thermal properties. The heat transfer capability is based on its property, dimensions, and volume fraction [10]. Because of that, nanofluids are promising cooling fluids for next-generation heat dispersants.

The nanofluids thermal conductivity is found to be an attractive property for many engineering applications. It represents the material ability to conduct or transmit heat. Much research has been conducted on measuring the nanofluid thermal conductivity. Most authors found that compared to base fluids, nanofluids deliver higher thermal conductivity. The thermal conductivity of nanofluids increases with an increase in particle size, stability, dispersion, temperature, and particle concentration. These variables play a very important role in determining the thermal conductivity of nanofluids [11]. Typical thermal conductivity enhancement is about 15 % over that of the base fluid and the heat transfer coefficient increases up to 40 % [10].

Production of nanoparticles is accomplished by one of the two ways: chemical processes and physical processes. Chemical processes include thermal spraying, spray pyrolysis, and chemical precipitation. Physical techniques include the inert gas condensation technique and mechanical grinding. Nanofluids are potential fluids of convective heat transfer with improved thermal properties and heat transfer performance. They can be used in a variety of devices for better performance i. e. convective heat transfer, energy, and so on [12]. This work is considered very novel since none of the studies in the literature have carried any of the geometrical and flow configurations for enhanced annular finned tube detection within a fluidic cell under a fluid-structure interaction model.

In this research, none of the previous studies have tackled the problem of fluid-heat-structure interaction between fluid flow, typical twisted tape insert, and this work paves the way for researchers to understand the mechanism of interaction in sciences and to study the effect of fluid flow, as well as the effect of temperature, (heat transfer) on the structure of objects (tube and tapes), called a one-way interaction, and the effect of deformation of the tube and tape as a result of expansion and pressure on the fluid direction and heat transfer with time (transient case), called a two-way interaction. In fact, it is necessary to conduct scientific research on this topic to give a real perception of what is happening between fluids and structures in the presence of heat, and neglecting this interaction process gives unreal results. The results of this study can give a real picture of the extent to which tubes can withstand strains and stresses before reaching the failure stage, and also enable us to predict the real processes of forced convection heat transfer on which most industrial processes depend.

---

## 2. Literature review and problem statement

---

There are two different fluid-structure interaction approaches, depending on the physical nature of the interaction, one-way and two-way coupled FSI. Recent progress in computing power has led to a great advance in computational fluid dynamics (CFD) and computational structural dynamics (CSD), so, many researchers are trying to solve the FSI problems by coupling the equation of motion for the fluid with that for the structure. The multi-physics phenomenon when a flow of fluid makes a deformation to the solid structure of a system, leading to changes in the system boundary conditions, is called fluid-structure interaction (FSI). In vice versa, when the solid structure around the fluid causes a change in fluid properties, this is also called FSI. This phenomenon may occur naturally or through engineering systems and becomes an essential matter in engineering systems design and analysis. In fact, it has a significant role in heat transfer processes. For most FSI problems, analytical solutions to the model equations are impossible to obtain, whereas laboratory experiments are limited in scope. Thus, to investigate the fundamental physics involved in the complex interaction between fluids and solids, numerical simulations may be employed. For the past ten years, simulations of multi-physics problems have become more important in the field of numerical simulations and analyses.

A huge number of experimental works have been done to improve the heat transfer fluid side; though, the related heat transfer characteristics and flow profiles in complex geometries still have to be confirmed. In fact, previous studies were concerned with the heat transfer process and its effect on the fluid or the structure, as the studies were done separately. The most important studies that are concerned with the effect of heat on the fluid inside heat exchangers can be stated as follows. The pressure drop and heat transfer enhancement of half-length twisted tape inserts in a U-bend double-pipe heat exchanger have been investigated experimentally [13]. The results were compared with the plain heat exchanger data and presented a 40 % increase in the heat transfer coefficient with half-length twisted tape inserts. The results also found that the performance of half-length twisted tape inserts in the U-bend heat exchanger was better than in the plain heat exchanger. The effect of nanofluids on heat trans-

fer augmentation was studied experimentally to calculate the laminar heat transfer performance and pressure drop of alumina nanofluid inside a circular finned tube under constant inlet temperature conditions [14]. For this purpose,  $\text{Al}_2\text{O}_3$  nanoparticles of 20 nm size were synthesized, characterized and dispersed in distilled water to formulate  $\text{Al}_2\text{O}_3$ /water nanofluid containing 3 and 5 % volume concentrations of nanoparticles. The thermophysical properties were calculated during the experiments at different volumes of fraction and validated. Experiments were carried out in the Reynolds number range of 678–2,033 with a tape twist ratio  $H/D=1.85$ . The effect of different volume concentrations on the friction factor and the coefficient of convective heat transfer was studied. The results show that the coefficient of convective heat transfer is enhanced by increasing the concentration and particle volume. Measurements show a 21–51 % enhancement in the average heat transfer coefficient with a volume concentration of 5 % and about a 19–38 % increase with a volume concentration of 3 % compared to distilled water. In addition, the average ratio of  $f_{nf}/f_{bf}$  was about 2.3 for 5 % volume concentration. Therefore, there is a significant increase in friction factor for nanofluids. Empirical correlations are developed to estimate the Nusselt number and friction factor validation for nanofluids.

The objectives of fluid-structure interaction have comparatively been less acclaimed in the literature, so, the number of publications dealing with it is limited. The following are some studies that focused on studying the effect of vibrations on structures only, and the influence of thermal stresses and strain on heat exchanger material. The fluid-structure interaction natural frequency inside a fluid transporting pipe system was investigated numerically using the element-free Galerkin method [15]. The equations of natural frequency under various ambient conditions were expressed during the simulation. Moreover, the first natural frequency equations are simplified in the status of various boundary conditions. The natural frequency was studied on a straight pipe fixed at both ends considering the Coriolis force, as an example. The four parameters (mass, hardness, length and velocity flow) are studied in a known boundary condition in detail, the four components relate to the natural frequency of the fluid transporting pipe system, and the results show that the influence of Coriolis force on natural frequency is unobtrusive. Then, they analyzed the connection in the natural frequency of the pipe system and that of the Euler beam.

Experimental and theoretical studies on the response of a thin-wall fluid transporting pipe due to forced vibration were made in [16]. The experimental work examined several ends of pipes supports, pinned-pinned, flexible-flexible, fixed-fixed and fixed-free. The theoretical work was performed using a FORTRAN computer language to calculate and analyze the natural frequencies, the corresponding mode shapes, pipe deformations, stresses and shell vibration modes creation in addition to the fluid flow properties and the fluid-structure interaction solution. The results showed close matching between experimental and theoretical works.

The current study focuses on the combination of two famous sciences of mechanical engineering (Power and Applied), so, the effect of temperature on the fluid and the structure will be studied together and simultaneously. Most of the previous studies were not able to study the effect of thermal stresses on the fluid and the structure together due to the lack of necessary tools. Modern simulation programs (Ansys Fluent) have provided a service to facilitate the task

of conducting the current study, and to give advanced and very important results that can serve in engineering applications. In fact, this study is the first of its kind at the present time, and there are no previous studies before this research, and the results obtained will contribute greatly to solving many engineering problems and developing appropriate solutions to them.

---

### 3. The aim and objectives of the study

---

The aim of the study is to develop a method for the simulation of horizontal finned tube structural member subjected to pressure loading using a two-way coupling FSI analysis and to investigate the structural response as well as a fluid response in the two-way coupling method.

To achieve this aim, the following objectives are accomplished:

- to study the effect of volume fraction and Reynolds number on the total deformation, stress, strain, stream lines, velocity profile and two-way fluid-structure interaction for distilled water and nanofluid;
- to study the effect of interaction between the working fluid and twisted tape and finned tube on metal deformation;
- to study the influence of interaction between the working fluid and twisted tape and finned tube on velocity vector and magnitude;
- the solid solution is structural deformation solved using the finite element method in ANSYS both static and transient structural analyses and the fluid field is solved by using finite volume CFD in ANSYS Fluent.

---

### 4. Materials and methods

---

The present work uses a full-length typical twisted tape with nanofluid and fluid-structure interaction. The key objective of this study is to analyze the flow by developing numerical investigation tools, fluid-structure interaction and heat transfer characteristics of nanofluid ( $\text{Al}_2\text{O}_3$ /water) in a horizontal circular finned tube fitted with typical twisted tape under laminar and turbulent flow at constant inlet temperature.

The system geometry for the current study involves an integral-finned tube, where the working fluid flows, together with a typical twisted tape insert. The dimensions of the finned tube as shown in Fig. 1 are 1,500 mm length and 22 mm inner diameter. 240 fins are used in total with 3 mm height for each one and the spacing between them is 4 mm. Fig. 2 illustrates the twisted tape inserted in a finned tube. ( $H$ ) refers to the axial length for a half-turn of the tape (180° turn of twisting) over ( $W$ ), which refers to the width of the tube or tape known as the twist ratio  $y$  as shown below:

$$y = \frac{H}{W}. \quad (1)$$

The twisted tape information is given in Table 1. The model is designed using SolidWorks computer program and meshed using ANSYS computer program.

The position of the structural member in the Computational Structural Mechanics (CSM) model is identical to the position of the model; otherwise, it would lead to errors while transferring data between two solvers.

Table 1

Dimensions of twisted tape insert

Twisted Tape Type	Twist Ratio ( $y$ )	Pitch ( $H$ ) (mm)	Width ( $W$ ) (mm)	Thickness ( $\delta$ ) (mm)
Typical	1.85	40.8	17.15	1

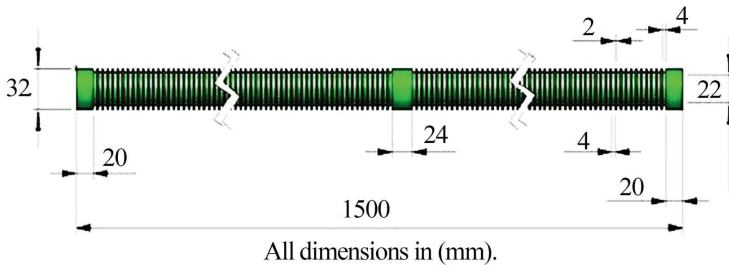


Fig. 1. Physical geometry of the finned tube

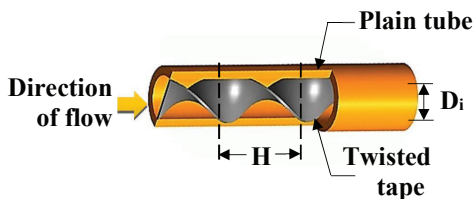


Fig. 2. Physical geometry of the tube and twisted tape [17]

The thermophysical properties are useful to define the nanofluid or base fluid that works inside the tube. To predict the effective thermal conductivity of nanofluids correctly, many empirical and theoretical models have been proposed. In this work, the Buongiorno model [18] is utilized to compute the nanofluid thermal conductivity as follows:

$$k_{nf} = k_{bf} (1 + 7.74\phi).$$

A new correlation form for Al<sub>2</sub>O<sub>3</sub>/water nanofluid was presented in the graphical form [19] and compared with various other models as follows:

$$\mu_{nf} = (1 + 7.3\phi + 123\phi^2) \mu_{bf}.$$

The nanofluid density can be calculated from the equation shown below:

$$\rho_{nf} = \left(\frac{m}{V}\right)_{nf} = \frac{\rho_{bf} V_{bf} + \rho_p V_p}{V_{bf} + V_p} = (1 - \phi) \rho_{bf} + \phi \rho_p.$$

The nanofluid specific heat can be computed by assuming thermal equilibrium between the base fluid and nanoparticles as follows:

$$Cp_{nf} = \frac{(1 - \phi) \rho_{bf} Cp_{bf} + \phi \rho_p Cp_p}{\rho_{nf}}.$$

The calculation of volume concentration for nanoparticles in the base fluid is performed by the following relation:

$$\phi\% = \frac{(m_p / \rho_p)}{(m_p / \rho_p) + (m_{bf} / \rho_{bf})}.$$

The nanofluid information is listed in Table 2.

These properties are entered into the database of the Fluent program in order to extract the solution.

The test tube geometry is divided into two parts. One part is the cylindrical tube with 1,500 mm length, 22 mm inner diameter, and 5 mm thickness. This part represents the outer design of the geometry. The tube has an integral fin as mentioned above. The tube was designed by SolidWorks computer program and created as a 3D geometry by Ansys Workbench. The method used to create the mesh is the unstructured meshing method, which meshed it into 68,069 nodes and 206,085 elements as illustrated in Fig. 3.

SolidWorks computer program was also used to design the twisted tape then ANSYS Workbench was used to create the 3D geometry. Patch independent tetrahedron is the meshing method used, and it meshed the twisted tape into 94,982 nodes and 43,054 elements as illustrated in Fig. 4.

Table 2

Nanofluid properties with different concentrations of Al<sub>2</sub>O<sub>3</sub>

Properties	$\phi=0\%$	$\phi=3\%$	$\phi=5\%$
$k_{nf}$ (W/m·K)	0.600	0.631	0.652
$\rho_{nf}$ (kg/m <sup>3</sup> )	998.2	1084.65	1142.29
$\mu_{nf}$ (Kg/m·s)	0.001002	0.001332	0.001676
$C_{p,nf}$ (J/kg K)	4,182	3816.16	3603.03
$k_{nf} / k_{bf}$	1	1.051	1.086
$\mu_{nf} / \mu_{bf}$	1	1.329	1.672

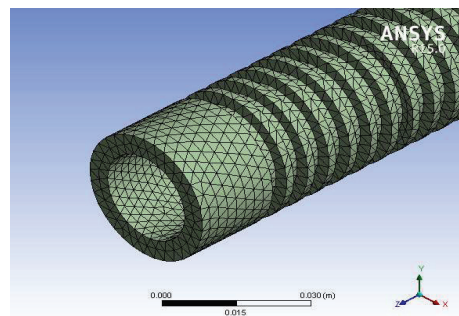


Fig. 3. Meshing of the plain tube geometry

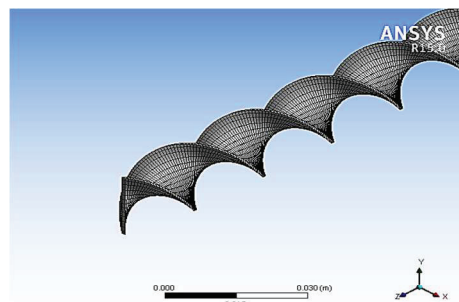


Fig. 4. Meshing of the twisted tape insert geometry

In this study, the triangular element type is employed for surface mesh and tetrahedron element type is used for three-dimensional geometry. This is because it has a priority in sophisticated geometries.

The flow in two ways is assumed to be laminar and turbulent flow. By this fact, the governing equations used

belong to these two-condition flows. The flow should follow the laws of mass conservation (continuity equation), momentum conservation, and energy conservation for the flow with the heat transfer process. For the flow of the nanofluid in two cases, every law will be written in two forms using Cartesian coordinate equations as follows (Governing equations in the laminar region).

The mass conservation equation (continuity equation) is obtained based on a constant mass (mass conservation) on a small differential volume.

$$\frac{\partial u}{\partial x} + \frac{\partial v}{\partial y} + \frac{\partial w}{\partial z} = 0.$$

The Newton's second law states "the variation of momentum on a fluid differential volume is equal to the total forces applied on this volume". By applying this law on a small differential nanofluid volume, the momentum equations could be derived. The Cartesian coordinate equations were converted to cylindrical coordinate by the Fluent package, so the equations in general are [20]:

–  $x$ -axis momentum equation:

$$\begin{aligned} \rho_{nf} \left( u \frac{\partial u}{\partial x} + v \frac{\partial u}{\partial y} + w \frac{\partial u}{\partial z} \right) &= \\ &= -\frac{\partial p}{\partial x} + \mu_{nf} \left( \frac{\partial^2 u}{\partial x^2} + \frac{\partial^2 u}{\partial y^2} + \frac{\partial^2 u}{\partial z^2} \right); \end{aligned}$$

–  $y$ -axis momentum equation:

$$\begin{aligned} \rho_{nf} \left( u \frac{\partial v}{\partial x} + v \frac{\partial v}{\partial y} + w \frac{\partial v}{\partial z} \right) &= \\ &= -\frac{\partial p}{\partial y} + \mu_{nf} \left( \frac{\partial^2 v}{\partial x^2} + \frac{\partial^2 v}{\partial y^2} + \frac{\partial^2 v}{\partial z^2} \right); \end{aligned}$$

–  $z$ -axis Momentum equation:

$$\begin{aligned} \rho_{nf} \left( u \frac{\partial w}{\partial x} + v \frac{\partial w}{\partial y} + w \frac{\partial w}{\partial z} \right) &= \\ &= -\frac{\partial p}{\partial z} + \mu_{nf} \left( \frac{\partial^2 w}{\partial x^2} + \frac{\partial^2 w}{\partial y^2} + \frac{\partial^2 w}{\partial z^2} \right). \end{aligned}$$

The first law of thermodynamics, which is known as energy conservation law states "the summation of rejected or added heat and the work done on fluid particle are equal to change in energy of it". Therefore, the equation is converted to the following form:

$$\begin{aligned} (\rho C_p)_{nf} \left( u \frac{\partial T_{nf}}{\partial x} + v \frac{\partial T_{nf}}{\partial y} + w \frac{\partial T_{nf}}{\partial z} \right) &= \\ &= K_{nf} \left( \frac{\partial^2 T_{nf}}{\partial x^2} + \frac{\partial^2 T_{nf}}{\partial y^2} + \frac{\partial^2 T_{nf}}{\partial z^2} \right). \end{aligned}$$

The feature of turbulent flows is oscillating velocity fields, the transported quantities such as particle concentration, energy, and momentum also oscillate and mix. Unfortunately, there is no ultimate turbulence model accepted for all cases of flow. Turbulence model can be chosen according to the assumption of the case such as the generated exercise for a specific case, the physics encompassed in the flow, the grade of accuracy needed, available computational resources, and time available for the simulation [21]. The continuity equation of turbulence flow is:

$$\frac{\partial \bar{u}}{\partial x} + \frac{\partial \bar{v}}{\partial y} + \frac{\partial \bar{w}}{\partial z} = 0.$$

The momentum equations for 3-dimensional turbulence flow are:

–  $x$ -axis momentum equation:

$$\begin{aligned} \left( \bar{u} \frac{\partial \bar{u}}{\partial x} + \bar{v} \frac{\partial \bar{u}}{\partial y} + \bar{w} \frac{\partial \bar{u}}{\partial z} \right) &+ \\ + \left( \frac{\partial}{\partial x} (\overline{u'^2}) + \frac{\partial}{\partial y} (\overline{u'v'}) + \frac{\partial}{\partial z} (\overline{u'w'}) \right) &= \\ = -\frac{1}{\rho_{nf}} \frac{\partial p}{\partial x} + \gamma \nabla^2 \bar{u}; \end{aligned}$$

–  $y$ -axis momentum equation:

$$\begin{aligned} \left( \bar{u} \frac{\partial \bar{v}}{\partial x} + \bar{v} \frac{\partial \bar{v}}{\partial y} + \bar{w} \frac{\partial \bar{v}}{\partial z} \right) &+ \\ + \left( \frac{\partial}{\partial x} (\overline{u'v'}) + \frac{\partial}{\partial y} (\overline{v'^2}) + \frac{\partial}{\partial z} (\overline{v'w'}) \right) &= \\ = -\frac{1}{\rho_{nf}} \frac{\partial p}{\partial y} + \gamma \nabla^2 \bar{v}; \end{aligned}$$

–  $z$ -axis momentum equation:

$$\begin{aligned} \left( \bar{u} \frac{\partial \bar{w}}{\partial x} + \bar{v} \frac{\partial \bar{w}}{\partial y} + \bar{w} \frac{\partial \bar{w}}{\partial z} \right) &+ \\ + \left( \frac{\partial}{\partial x} (\overline{u'w'}) + \frac{\partial}{\partial y} (\overline{v'w'}) + \frac{\partial}{\partial z} (\overline{w'^2}) \right) &= \\ = -\frac{1}{\rho_{nf}} \frac{\partial p}{\partial z} + \gamma \nabla^2 \bar{w}. \end{aligned}$$

And the energy equation for turbulence flow is:

$$\begin{aligned} \left( \bar{u} \frac{\partial \bar{T}_{nf}}{\partial x} + \bar{v} \frac{\partial \bar{T}_{nf}}{\partial y} + \bar{w} \frac{\partial \bar{T}_{nf}}{\partial z} \right) &= \\ = \alpha \nabla^2 \bar{T}_{nf} + \left( -\frac{\partial}{\partial x} (\overline{u'T'_{nf}}) - \frac{\partial}{\partial y} (\overline{v'T'_{nf}}) - \frac{\partial}{\partial z} (\overline{w'T'_{nf}}) \right). \end{aligned}$$

The eddy viscosity distribution in the domain of flow must be created so as to compute the momentum and coefficients of heat diffusion for turbulent equations. This is the turbulent model job. The realizable  $k$ - $\epsilon$  model (RKE) was used in the present work [22], which provides better performance for flows involving thermal boundary layers, rotation, separation, and recirculation [23]. The turbulence kinetic energy,  $k$ , and its dissipation rate  $\epsilon$ , are obtained from the following equations:

$$\begin{aligned} \frac{\partial}{\partial t} (\rho_{nf} k) + \frac{\partial}{\partial x_i} (\rho_{nf} k u_i) &= \\ = \frac{\partial}{\partial x_j} \left[ \left( \mu + \frac{\mu_t}{\sigma_k} \right) \frac{\partial k}{\partial x_j} \right] + G_k + G_b - \rho_{nf} \epsilon - Y_M + S_k, \\ \frac{\partial}{\partial t} (\rho_{nf} \epsilon) + \frac{\partial}{\partial x_i} (\rho_{nf} \epsilon u_i) &= \frac{\partial}{\partial x_j} \left[ \left( \mu + \frac{\mu_t}{\sigma_k} \right) \frac{\partial \epsilon}{\partial x_j} \right] + \\ + C_{1\epsilon} \frac{\epsilon}{k} (G_k + C_{3\epsilon} G_b) - C_{2\epsilon} \frac{\epsilon^2}{k} + S_\epsilon. \end{aligned}$$

In the analysis of FSI, there is loads transfer from the structure and fluid at the interface and vice versa. In this case, boundary conditions have been changed and the mesh was updated at every step of the analysis. In the fluid, the conservation of mass equation is the same, but as the solution domain keeps changing every time, the general momentum equation cannot be used in transient analysis, so as the flow boundary changed the grid has to be updated [24]. Thus, the equation of momentum is changed so the grid is subject to updating all the time, which is given by equation 20 for the  $i^{th}$  element:

$$\frac{\partial}{\partial t} \int_{\Omega} \rho \partial \Omega + \int_S \rho (\mathbf{v} - \mathbf{v}_b) n dS = \int_S (\tau_{ij} i_j - P_{ij}) n dS + \int_{\Omega} b_i \partial \Omega.$$

The calculations for the structure side are based on impulse conservation. It is solved using a finite element approach, where a finite element is chosen for each specific problem.

$$[M]\{\ddot{U}\} + [C]\{\dot{U}\} + [K]\{U\} = \{F\}.$$

Transient dynamic analysis is conducted to find the structure dynamic response when subjected to time-dependent loads.

### 5. Numerical test rig data verification

The Nusselt number numerical results of the tube induced with a plain twisted tape insert were validated with a correlation derived by Hong and Bergles [25]. Fig. 5 shows the validation results of the average Nusselt number between numerical results of the typical twisted tape insert (TT) and Hong and Bergles correlation. The experimental results are in good agreement with the experimental data and fall within a deviation of 12 %.

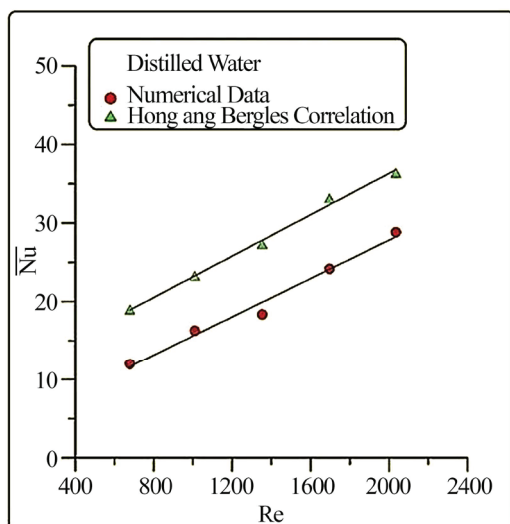


Fig. 5. Validation of  $(\overline{Nu})$  with numerical data for laminar flow regime

## 6. Simulation results

### 6.1. Effect of volume concentration on total deformation

In Fig. 6, the displacement is shown at six time periods for nanofluid at laminar flow conditions and volume concentration of 3 %. The load of pressure increases linearly up to 0.125 seconds. From this time period until 0.98 seconds and onward, maximum deformation occurred due to full load applying. This case shows that the deformations of two-way coupling fluctuate back and forth, with higher amplitude of 0.004 mm. Fig. 7 shows the total deformation for nanofluid under a turbulent flow regime with a volume concentration of 5 %. The maximum amplitude is 0.0033 mm.

The two-way simulations show an interesting observation that the maximum deformation is located at the center of the twisted tape.

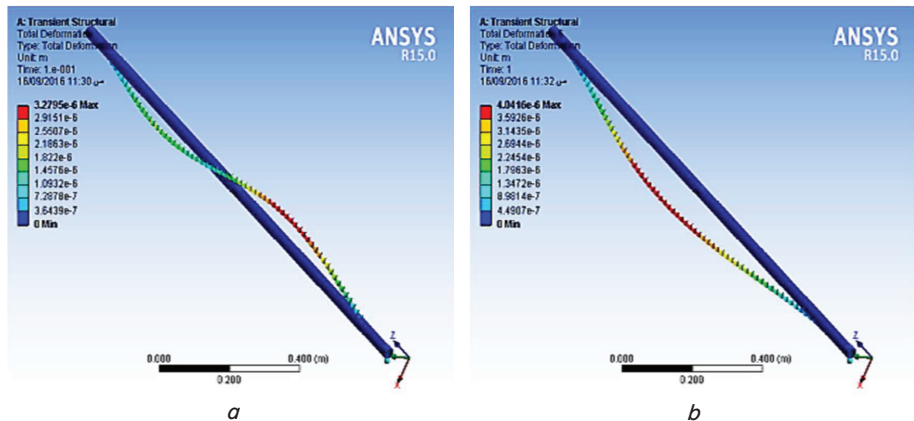


Fig. 6. Transient deformation during 1 second at  $Re=679$  and  $\phi=3\%$ : a – 0.1 s; b – 1 s

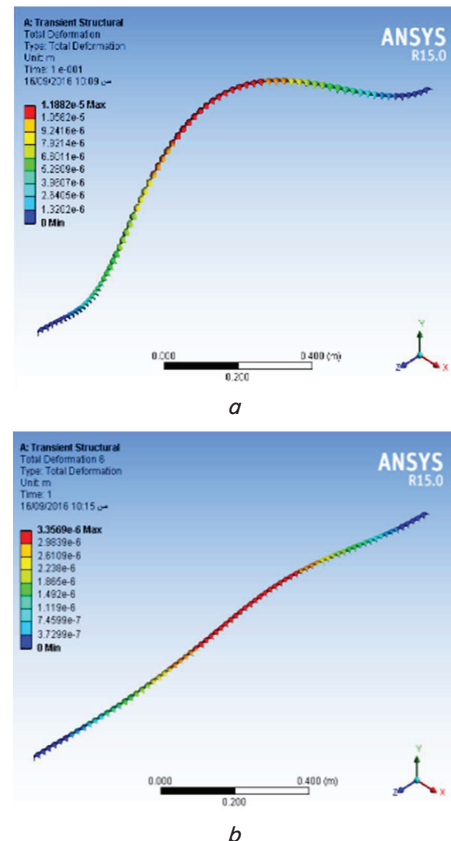


Fig. 7. Transient deformation for six periods at  $Re=3391$  and  $\phi=5\%$ : a – 0.1 s; b – 1 s

### 6.2. Effect of interaction on stress distribution

The maximum von Mises stress has moderate fluctuations between every iteration of coupling. Fig. 8 demonstrates the von Mises stress distribution on the twisted tape for alumina nanofluid at  $\phi=3\%$  and  $Re=679$ . The higher stress for the twisted tape insert is 0.098 MPa at a period of 0.01 sec, but the minimum stress for the tape is 0.02 Pa at a time period of 0.13 sec. Fig. 9 shows the equivalent (von Mises) stress for nanofluid under turbulent flow regime. The maximum stress value in the turbulent condition is 0.13 MPa at a volume concentration of 5%.

The two-way simulations show an interesting observation that the maximum stress is located on both ends of the twisted tape.

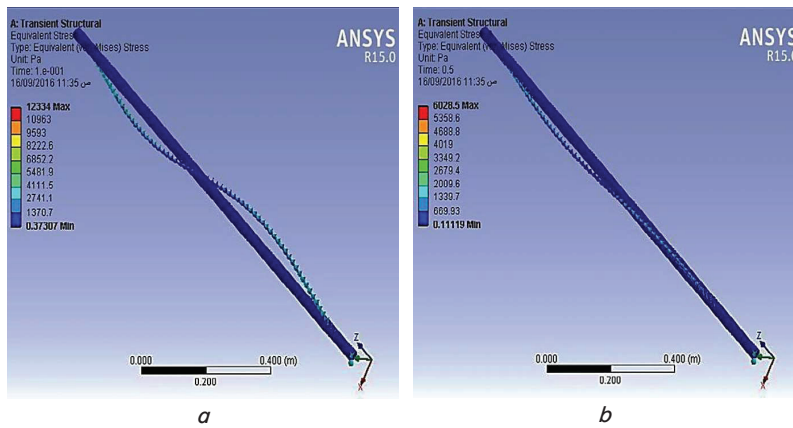


Fig. 8. Equivalent stress for half-second at  $Re=679$  and  $\phi=3\%$ :  $a - 0.1\text{ s}$ ;  $b - 0.5\text{ s}$

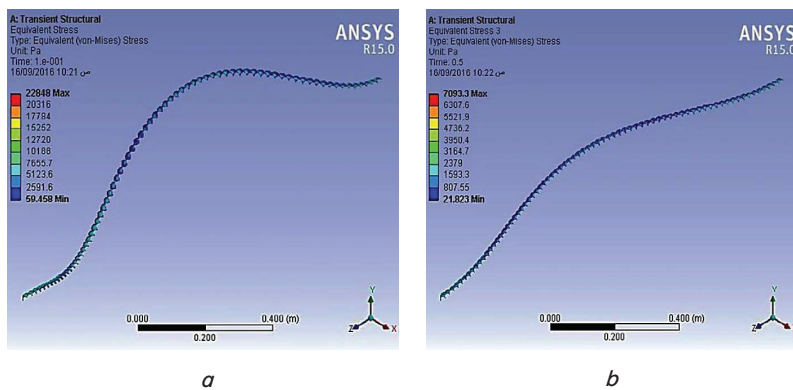


Fig. 9. Equivalent stress for three periods at  $Re=3,391$ :  $a - 0.1\text{ s}$ ;  $b - 0.5\text{ s}$

### 6.3. Effect of interaction on strain distribution

The equivalent elastic strain distribution on the typical twisted tape insert for nanofluid at a concentration  $\phi=3\%$  is shown in Fig. 10. The higher strain is 0.0000013 m/m at a period of 0.01 sec. From this figure, we can see that the highest strain occurs in the tape central region. Fig. 11 shows the equivalent elastic strain for nanofluid under turbulent flow regime. The maximum elastic strain in turbulent flow is 0.00000012 m/m at a volume concentration of 5%.

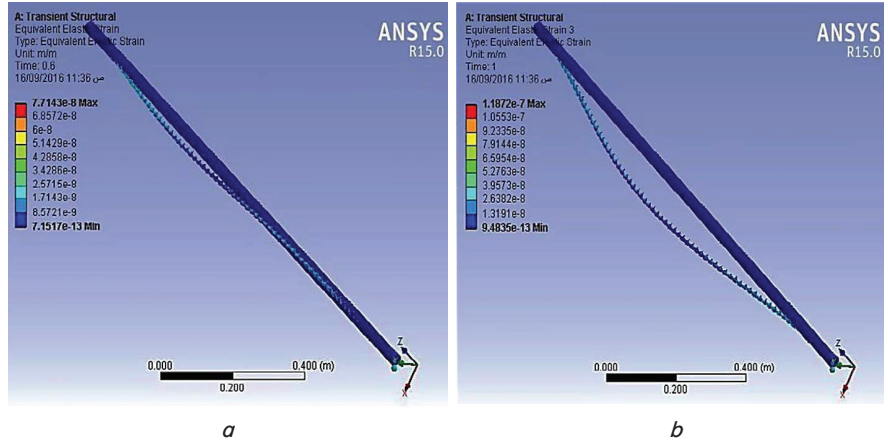


Fig. 10. Equivalent strain for three periods at  $Re=679$  and  $\phi=3\%$ :  $a - 0.6\text{ s}$ ;  $b - 1\text{ s}$

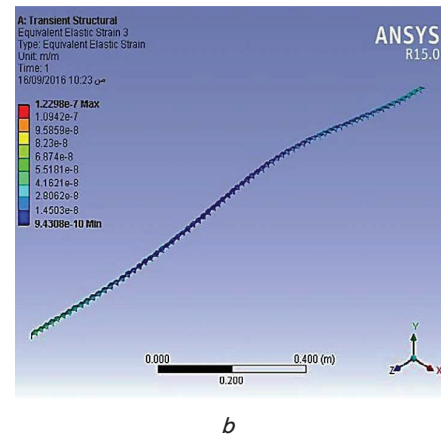
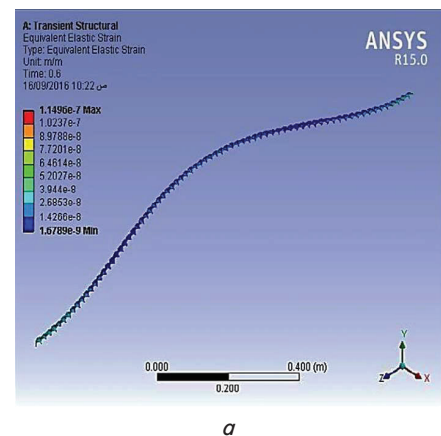


Fig. 11. Equivalent strain for three periods at  $Re=3,391$  and  $\phi=5\%$ :  $a - 0.6\text{ s}$ ;  $b - 1\text{ s}$

The two-way simulations show an interesting observation that the maximum strain is located at the center of the twisted tape.

### 6.4. Effect of interaction on velocity and vectors distribution

Fig. 12 depicts a 3D view of typical twisted tape with contours of velocity along the test section for alumina nanofluid in two-way interaction with the coupling system for laminar flow regime. The CFD-Post picture shows that the velocity value changes with time transiently, because the direction of the velocity change is due to the reaction force of the twisted tape. Fig. 13 demonstrates the velocity contours

along the test section for nanofluid in two-way interaction with the coupling system, under turbulent flow regime. The CFD-Post picture shows the same change in direction and magnitude, as mentioned in the previous paragraph. Fig. 14, 15 highlight a 3D view of a typical twisted tape insert with velocity vector along the test section for nanofluid at a volume of fraction of 3 % and 5 %, respectively.

to the twisted tape deformation effect, which is much higher than that of the rigid flat tube, result from elongation, effect of fluid pressure and its reaction force.

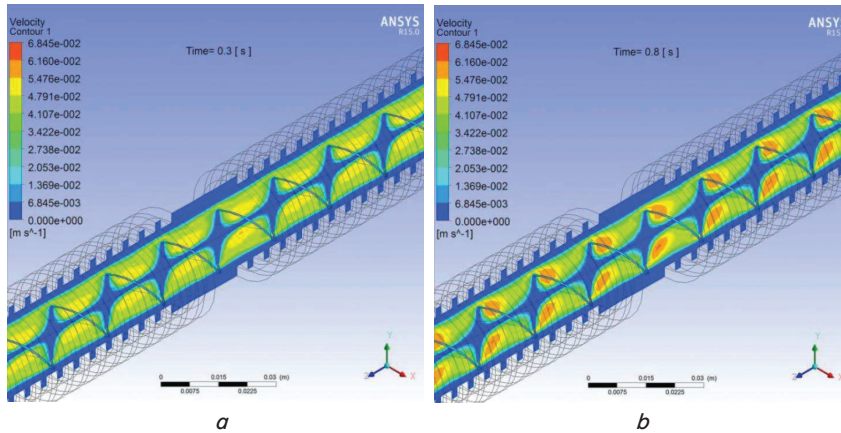


Fig. 12. Velocity contours for two periods at  $Re=679$  and  $\varphi=3\%$ : a – 0.3 s; b – 0.8 s

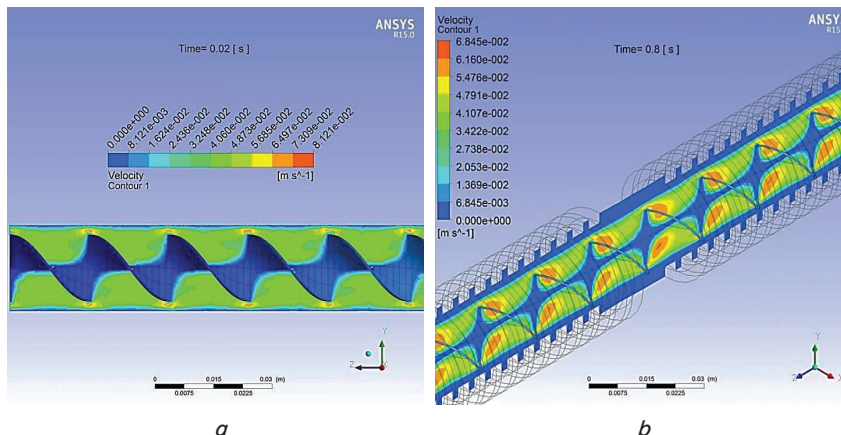


Fig. 13. Velocity contours for two periods at  $Re=3,391$  and  $\varphi=5\%$ : a – 0.02 s; b – 0.8 s

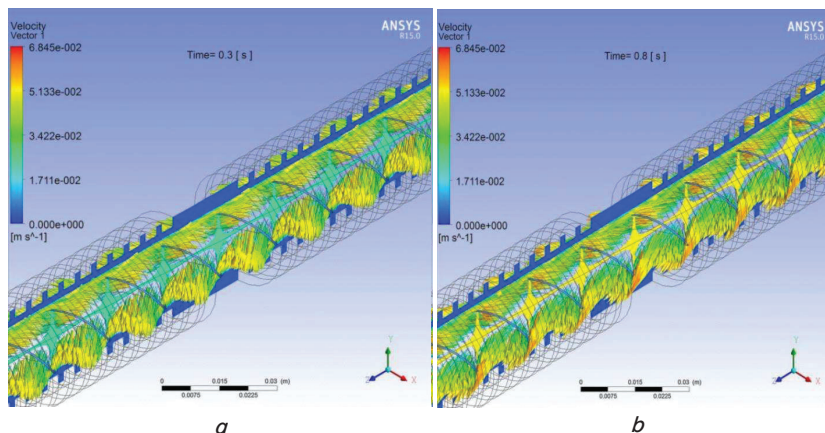


Fig. 14. Velocity vectors for two time periods at  $Re=679$  and  $\varphi=3\%$ : a – 0.3 s; b – 0.8 s

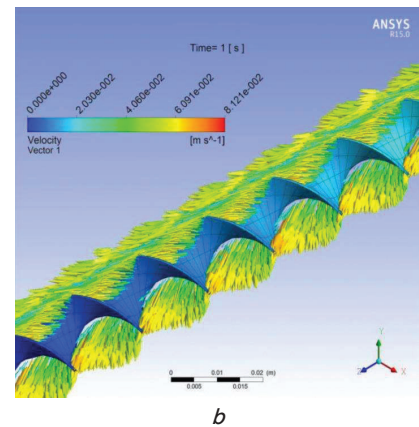
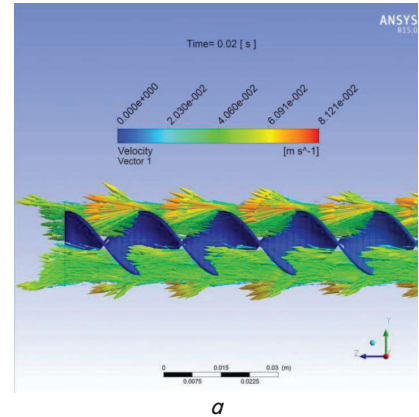


Fig. 15. Velocity vectors for two time periods at  $Re=3,391$  and  $\varphi=5\%$ : a – 0.02 s; b – 1 s

## 7. Discussion of simulation results

In this research, numerical results are presented and discussed to indicate the reasons behind such results. They include the tests of both water and nanofluid in a horizontal tube with twisted tape using a twist ratio  $TR=1.85$  and nanofluid concentrations  $\varphi=3, 5\%$  by volume. Numerical results included also those situations that are difficult or impossible to measure with the available equipment, especially Fluid-Heat-Structure Interaction (FHSI).

To examine the effect of nanofluid on the total deformation, we can observe that the deformation of the twisted tape is the result of constant heat flow. The heat is transferred through the tube to the conveying fluid and then to the twisted tape, which leads to an increase in the temperature of the twisted tape and the force of water pushing on the tape and the reaction resulting from this force will lead to deformation in the metal of the twisted tape. As for adding nanofluids

From these figures, we can observe that the vector magnitude and its direction change at different time periods due

reaction resulting from this force will lead to deformation in the metal of the twisted tape. As for adding nanofluids



to the water, the fluid temperature will decrease due to the ability of these particles to draw heat to the outside, which leads to a decrease in the surface temperature of the tape. Therefore, the force of the flow does not significantly affect the tape upon collision. It can also be noted that the reason for the deformation is concentrated in the center of the tube is that the twisted tape behaves as a simply supported beam fixed on both sides, therefore, the deformation is large in the center due to the free movement of the tape.

For the influence of interaction on thermal stresses, the addition of nanofluids to the water leads to an increase in the force of gravity of the fluid, and thus the force of collision with the twisted tape decreases, which leads to a reduction in the stress on the tape. It can also be seen that the stress value is high at the beginning due to the reaction strength of the tape metal, which gradually decreases with time, and that the highest stress is at the fixed sides because of the resultant reaction force and that the least stress is in the center of the twisted tape because of the freedom of movement in this area. In the case of turbulent flow, the stress value increases with the increase in the nanofluid concentration due to the high velocity of water inside the tube, which overcomes the force of gravity, which leads to an increase in the force exerted on the tape and thus an increase in the force exerted on the unit area.

The influence of interaction on strain distribution is illustrated as follows, the value of the strain decreases with increasing nanofluid concentrations for the reasons mentioned in stress condition. However, the maximum value of the strain is in the center of the tape, unlike the stress that is concentrated on the edges due to the freedom of movement of the tape in this region, which leads to a change in the length of the tape relative to its original length.

Velocity contours and vectors demonstrate the effect of interaction on the magnitude and direction of motion based on the presence of the nanofluid and the increase in the mass flow rate inside the tube. The force of the fluid collision with

the tape and the reaction resulting from the collision led to a significant change in the velocity direction with time, and the presence of the nanofluid has led to back flow, especially in the sharp edges of the twisted tape and at the tube ends.

The advantage of this study is clarified real interaction that occurs between the fluid and the structure from action and reaction and its effect on the values of stress, strain and deformation in addition to the effect of temperature on the fluid and the structure (tube and twisted tape) at the same time without separating the two effects as was happening in previous studies. But the drawback of this study is that the simulation tool needs additional development, since the simulation process takes a very long time to extract the results and study them due to the difficulty of the cases.

---

## 7. Conclusions

---

1. The total deformation was affected by nanofluid addition and its influence was concentrated at the center of the twisted tape, and the maximum deformation was 0.004 mm.
2. The stress value was affected by an increase in Reynolds number, and its highest effect was at the edges of the twisted tape, and its magnitude was 0.098 MPa.
3. The strain value was also affected by adding nanofluid and increasing Reynolds number, and its highest value was in the middle of the tape, and its magnitude was 0.0000013 m/m.
4. The velocity magnitude and direction change due to the reaction force of the twisted tape, and the maximum change was in the case of turbulent flow.

---

## Acknowledgments

---

The authors wish to thank Dr. Mohammed Mousa for his continued support of this research.

---

## References

1. Johar, G. (2010). Experimental Studies on Heat Transfer Augmentation Using Modified Reduced Width Twisted Tapes (RWTT) as Inserts for Tube Side Flow of Liquids. National Institute of Technology, Rourkela. Available at: [http://ethesis.nitrkl.ac.in/1842/1/Gaurav\(10600023\)\\_Virendra\(10600006\)\\_ethesis.pdf](http://ethesis.nitrkl.ac.in/1842/1/Gaurav(10600023)_Virendra(10600006)_ethesis.pdf)
2. Bergles, A. E.; Bohsenow, W. M., Hartnett, J. P., Cho, Y. I. (Eds.) (1998). Techniques to augment heat transfer. In "Handbook of Heat Transfer". Ch. 11. McGraw-Hill.
3. Manglik, R. M. (2003). Heat transfer enhancement. In Heat Transfer Handbook. Ch. 14. Wiley, 1029–1130. Available at: [https://www.academia.edu/13224136/Heat\\_Transfer\\_Handbook](https://www.academia.edu/13224136/Heat_Transfer_Handbook)
4. Siddique, M., Khaled, A.-R. A., Abdulhafiz, N. I., Boukhary, A. Y. (2010). Recent Advances in Heat Transfer Enhancements: A Review Report. International Journal of Chemical Engineering, 2010, 1–28. doi: <https://doi.org/10.1155/2010/106461>
5. You, L. (2002). Computational Modeling of Laminar Swirl Flows and Heat Transfer in Circular Tubes with Twisted-Tape Inserts. University of Cincinnati, 95. Available at: [https://etd.ohiolink.edu/apexprod/rws\\_olink/r/1501/10?p10\\_etd\\_subid=79049&clear=10#abstract-files](https://etd.ohiolink.edu/apexprod/rws_olink/r/1501/10?p10_etd_subid=79049&clear=10#abstract-files)
6. Elshafei, E. A. M., Safwat Mohamed, M., Mansour, H., Sakr, M. (2008). Experimental study of heat transfer in pulsating turbulent flow in a pipe. International Journal of Heat and Fluid Flow, 29 (4), 1029–1038. doi: <https://doi.org/10.1016/j.ijheatfluidflow.2008.03.018>
7. Liu, S., Sakr, M. (2013). A comprehensive review on passive heat transfer enhancements in pipe exchangers. Renewable and Sustainable Energy Reviews, 19, 64–81. doi: <https://doi.org/10.1016/j.rser.2012.11.021>
8. Choi, S. U. S. (2008). Nanofluids: A New Field of Scientific Research and Innovative Applications. Heat Transfer Engineering, 29 (5), 429–431. doi: <https://doi.org/10.1080/01457630701850778>
9. Pfautsch, E. (2008). Forced Convection in Nanofluids over a Flat Plate. University of Missouri. doi: <https://doi.org/10.32469/10355/5745>

10. Usri, N. A. B. (2010). Experimental Study of Heat Transfer Coefficient for Nanofluid with Inserted Tape. Universiti Malaysia Pahang. Available at: [http://umpir.ump.edu.my/id/eprint/1905/1/Nur\\_Ashikin\\_Usri\\_\(CD\\_4989\\_\).pdf](http://umpir.ump.edu.my/id/eprint/1905/1/Nur_Ashikin_Usri_(CD_4989_).pdf)
11. Rudyak, V. Y., Belkin, A. A., Tomilina, E. A. (2010). On the thermal conductivity of nanofluids. *Technical Physics Letters*, 36 (7), 660–662. doi: <https://doi.org/10.1134/s1063785010070229>
12. Saidur, R., Leong, K. Y., Mohammed, H. A. (2011). A review on applications and challenges of nanofluids. *Renewable and Sustainable Energy Reviews*, 15 (3), 1646–1668. doi: <https://doi.org/10.1016/j.rser.2010.11.035>
13. Yadav, A. S. (2009). Effect of Half Length Twisted-Tape Turbulators on Heat Transfer and Pressure Drop Characteristics inside a Double Pipe U-Bend Heat Exchanger. *Jordan Journal of Mechanical and Industrial Engineering*, 3 (1), 17–22. Available at: [https://www.researchgate.net/publication/237250067\\_Effect\\_of\\_Half\\_Length\\_Twisted-Tape\\_Turbulators\\_on\\_Heat\\_Transfer\\_and\\_Pressure\\_Drop\\_Characteristics\\_inside\\_a\\_Double\\_Pipe\\_U-Bend\\_Heat\\_Exchanger](https://www.researchgate.net/publication/237250067_Effect_of_Half_Length_Twisted-Tape_Turbulators_on_Heat_Transfer_and_Pressure_Drop_Characteristics_inside_a_Double_Pipe_U-Bend_Heat_Exchanger)
14. Habeeb, L. J., Saleh, F. A., Maajel, B. M. (2017). Experimental investigation of laminar convective heat transfer and pressure drop of AL2O3/water nanofluid in circular tube fitted with twisted tape insert. *International Journal of Energy Applications and Technologies*, 4 (2), 73–86. Available at: <https://dergipark.org.tr/en/download/article-file/333724>
15. Yi-min, H., Yong-shou, L., Bao-hui Li, Yan-jiang, L., Zhu-feng, Y. (2010). Natural frequency analysis of fluid conveying pipeline with different boundary conditions. *Nuclear Engineering and Design*, 240 (3), 461–467. doi: <https://doi.org/10.1016/j.nucengdes.2009.11.038>
16. Mahmood, N. (2011). Study of the Response of a Conduit Conveying Fluid Due to a Forced Vibration. University of Technology, 198.
17. Habeeb, L., Saleh, F., Maajel, B. (2019). CFD modeling of laminar flow and heat transfer utilizing Al2O3/water nanofluid in a finned-tube with twisted tape. *FME Transactions*, 47 (1), 89–100. doi: <https://doi.org/10.5937/fmet1901089h>
18. Buongiorno, J. (2006). Convective Transport in Nanofluids. *Journal of Heat Transfer*, 128 (3), 240–250. doi: <https://doi.org/10.1115/1.2150834>
19. Wang, X., Xu, X., Choi, S. U. S. (1999). Thermal Conductivity of Nanoparticle - Fluid Mixture. *Journal of Thermophysics and Heat Transfer*, 13 (4), 474–480. doi: <https://doi.org/10.2514/2.6486>
20. ANSYS FLUENT 12.0 Theory Guide (2009). ANSYS, Inc. Available at: [https://www.afs.enea.it/project/neptunius/docs/fluent/html/th/main\\_pre.htm](https://www.afs.enea.it/project/neptunius/docs/fluent/html/th/main_pre.htm)
21. Shih, T.-H., Liou, W. W., Shabbir, A., Yang, Z., Zhu, J. (1995). A new k- eddy viscosity model for high reynolds number turbulent flows. *Computers & Fluids*, 24 (3), 227–238. doi: [https://doi.org/10.1016/0045-7930\(94\)00032-t](https://doi.org/10.1016/0045-7930(94)00032-t)
22. ANSYS FLUENT 12.0 User's Guide (2009). ANSYS, Inc. Available at: [https://www.afs.enea.it/project/neptunius/docs/fluent/html/ug/main\\_pre.htm](https://www.afs.enea.it/project/neptunius/docs/fluent/html/ug/main_pre.htm)
23. Benra, F.-K., Dohmen, H. J., Pei, J., Schuster, S., Wan, B. (2011). A Comparison of One-Way and Two-Way Coupling Methods for Numerical Analysis of Fluid-Structure Interactions. *Journal of Applied Mathematics*, 2011, 1–16. doi: <https://doi.org/10.1155/2011/853560>
24. Gambill, W. R., Bundy, R. D. (1962). An Evaluation of the Present Status of Swirl-Flow Heat Transfer. ASME Paper No. 62-HT-42, pp. 1–12.
25. Hong, S. W., Bergles, A. E. (1976). Augmentation of Laminar Flow Heat Transfer in Tubes by Means of Twisted-Tape Inserts. *Journal of Heat Transfer*, 98 (2), 251–256. doi: <https://doi.org/10.1115/1.3450527>